Chapter 17

New Injectors: The Linac4 Project and the New H^- Source

J. Lettry[1] and M. Vretenar[2]

[1]*CERN, BE Department, Genève 23, CH-1211, Switzerland*
[2]*CERN, Accelerator and Technology Sector, Genève 23, CH-1211, Switzerland*

Linac4 is a new 160 MeV linear accelerator designed to improve by a factor of 2 the beam brightness out of the LHC injection chain for the needs of the LHC luminosity upgrade. The project started in 2008 and beam commissioning takes place in 2014–2015. The new linac accelerates H^- ions that are then stripped at injection into the PS Booster; production of the H^- beam takes place in a state-of-the-art ion source of the RF-driven caesiated surface type. Acceleration is provided by four different accelerating sections matched to the increasing beam velocity, including two of novel designs, and focusing is provided by a combination of permanent-magnet and electromagnetic quadrupoles.

1. Introduction

The idea of building a new linear accelerator to make the LHC injectors capable of producing higher brightness beams dates back to the late 90s [1]: at that time the LHC was intended to start at full energy in 2008 and preparing for a high luminosity upgrade after about 10 years of operation was considered an utmost priority. In this perspective, the construction of some new accelerator was unavoidable: although successful, the program for the upgrade of the LHC injectors that took place in 1993–2000 in view of enabling the "nominal" LHC luminosity (10^{34} $cm^{-2}s^{-1}$) showed inherent limitations in the LHC injection chain that would not allow reaching the "ultimate" luminosity of 2.5×10^{34} $cm^{-2}s^{-1}$ or beyond [2]. Beam brightness from the injectors being one of the main factors limiting the LHC luminosity several upgrades of the injectors were considered; they all had in common a new linac of energy higher than the present 50 MeV of Linac2, the first bottleneck for higher brightness being the limitation to the intensity at injection into the PS Booster (PSB) due to space charge induced tune shift at 50 MeV [3]. Whereas initial upgrade plans concentrated on a high-energy linac, the SPL (Superconducting Proton Linac) that would inject into the PS a beam at 2.2 GeV energy thus overcoming both PSB and PS limitations [4], at a

later stage priority was given to a less ambitious program, based on the construction of a new linac injecting into the PSB at higher energy coupled with an increase of the PSB energy. The new linac was called Linac4, being the fourth hadron linac to be built at CERN [5]; after analyzing different options, the Linac4 energy was eventually fixed to 160 MeV, corresponding to a factor of 2 in $\beta\gamma^2$ with respect to the present 50 MeV injection (with β, γ relativistic beam parameters). Space charge induced tune shift scaling as $1/\beta\gamma^2$, the same tune shift as with Linac2 could be expected with twice the intensity in the same PSB transverse emittance, making possible a gain in brightness by a factor of 2. The Linac4 Technical Design Report was presented in 2006 [6] and construction of the new linac was approved by the CERN Council in June 2007; the project officially started in January 2008. After completing the civil engineering, the infrastructure and the construction of the machine components, beam commissioning has started in 2013 and will continue until end of 2015. Connection to the PSB will be possible from end of 2016.

Together with the increase in brightness for the LHC, the new linac is expected to bring other advantages to the CERN injector complex. The use of charge exchange injection in the PSB made possible by the acceleration in Linac4 of H^- ions instead of protons is expected to simplify the injection process reducing at the same time beam loss and activation; the modern construction technology of Linac4 will remove the concerns for long-term reliability related to the aging vacuum structure of Linac2; finally, a higher beam intensity will be available for non-LHC users of the PSB. As an additional feature, the Linac4 accelerator is designed to be able to operate at higher duty cycle than what was required by the PSB, following an upgrade of the power converters and of electrical and cooling infrastructure. This would make possible a future upgrade to become the injector for the proton driver accelerator of a neutrino facility.

2. Parameters, General Design and Layout

The main Linac4 parameters are reported in Table 1.

The new linac is dimensioned to double the maximum intensity from the PSB with the same transverse emittances, providing up to 10^{14} protons per pulse; it is expected to supply this charge with 400 μs long pulses at 40 mA current. The pulse repetition frequency is limited to a maximum of about 1 Hz by the PSB magnetic cycle, giving a beam duty cycle of less than 1%. In case Linac4 would be used in a future high-intensity facility for neutrino physics, the accelerating structures have been designed for a maximum duty cycle of 10%; infrastructure and power supplies are dimensioned only for the low duty cycle. About 35% of

Table 1. Main Linac4 design parameters.

Output energy	160	MeV
Bunch frequency	352.2	MHz
Repetition frequency	1.1 (max. 2)	Hz
Beam pulse length	0.4	ms
Beam duty cycle	0.08	%
Chopper beam-on rate	62	%
Linac pulse current	40	mA
N. of particles per pulse	1.0	$\times 10^{14}$
Transverse emittance	0.4	π mm mrad
Maximum RF duty cycle	10	%

the beam is chopped at 3 MeV and sent to a collimator/dump to allow low-loss capture of the beam in the PSB: this requirement together with some beam loss expected at low energy brings the required current out of the ion source to 80 mA. The RF frequency has been fixed at 352.2 MHz as in the old LEP accelerator, in order to recuperate klystrons and other RF equipment while remaining in the optimum frequency range for modern linear accelerators. The linac is composed of a 3 MeV injector followed by three different accelerating structures bringing the energy up to 160 MeV, for a total length of 75 m (Fig. 1).

The 3 MeV section is made of the ion source, of a Low Energy Beam Transport (LEBT), of a 3 m long Radio Frequency Quadrupole (RFQ) and of a 3.6 m long chopping and matching line that prepares the beam to be injected into the main accelerating structures. The three accelerating structures are a Drift Tube Linac (DTL) that reaches 50 MeV energy with three tanks, followed by a sequence of 7 Cell-Coupled Drift Tube Linac (CCDTL) modules going up to 104 MeV, and finally by 12 Pi-Mode Structure (PIMS) cavities reaching the final energy. All accelerating structures are normal conducting, the investment for superconducting accelerating structures not being justified in this range of energy and duty cycle, and have the same RF frequency to reduce cost and simplify

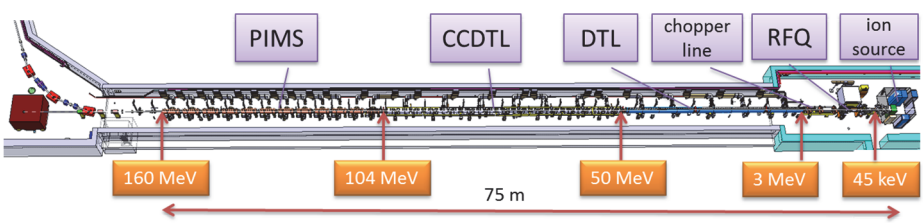

Fig. 1. Linac4 layout.

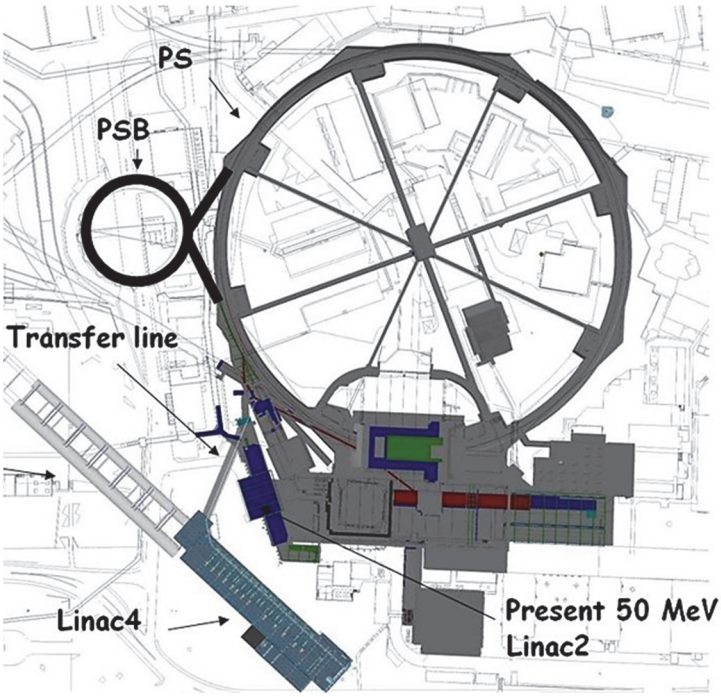

Fig. 2. Side and 2D view of tunnel and surface building.

maintenance thanks to standardised RF systems. A bending magnet at the end of the linac can send the beam to a transfer line connected to the existing Linac2 to PSB transfer line; beam diagnostics elements and a beam dump are placed in a straight line after the bending. The basic Linac4 layout is presented in Fig. 1, while Fig. 2 shows the location of Linac4 with respect to PSB, PS and Linac2.

3. Challenges of the Ion Source

The Linac4 requires the development of a completely new H^- source or at least a serious upgrade of the nearest existing design. None of the four H^- ion production mechanisms that were successfully demonstrated so far and operated in linear accelerator ion sources matches the specified duty-factor, emittance and ion beam current criteria at the 45 kV voltage required to inject into the RFQ. Additionally, for reliable operation for the LHC, Mean Time Between Maintenance (MTBM) driving factors such as sparking, material sputtering or contaminants should be identified and modeled and their detrimental effects minimized. Common feature to all H^- ion sources, the electrons co-extracted with the H^- beam must be properly dumped.

The H^- production mechanism taking place in the volume of the hydrogen plasma relies on the dissociation of an excited H_2^{ν} molecule by a low energy electron in the vicinity of the extraction region. This ion source does not require cesium to operate; this is a particularly valuable asset during test periods that may be more prone to non-nominal operation conditions. A challenging feature of volume sources is their large amount of co-extracted electrons (typ. e/H^- ratio of 30).

Cesium is a highly reactive alkali, requiring particularly low levels of oxygen or water vapor levels, it is an outstanding electron donor and in the seventies, its admixture to hydrogen discharge sources opened the path to larger H^- ion currents [7] while sizably reducing co-extracted electrons. In penning or magnetron discharge ion sources 0.3 to 3 g of metallic cesium is injected monthly; sputtering induced by the presence of hydrogen and Cs in the discharge electrical field is a relevant wear mechanism [8, 9].

An alternative design has been demonstrated by the SNS ion source team; in their RF sustained plasma ion source, a mono-layer of cesium deposited on their molybdenum extraction surface was providing a stable 60 mA beam of H^- for a period of five weeks at a record duty factor of 6% [10]. This caesiated surface mode of production reduces the average Cs consumption by 2 orders of magnitude and keeps a low e/H^- ratio. The hydrogen plasma of the SNS ion source is sustained by an internal solenoid RF system but a prototype with an external solenoid was also successfully operated for four weeks at SNS [11].

On the basis of today's state of the art H^- source designs/knowledge, the strategy decided for Linac4 has been to build an H^- volume source dedicated to low current tests and RFQ/Chopper commissioning while an H^- caesiated surface source driven by an external RF antenna solenoid is used for Linac4

Table 2. Summary of ion source parameters for the most representative ion sources operated at accelerator facilities for each of the H^- ion production mechanism; Volume, cesiated surface, Penning and Magnetron discharge [12, 13, 14].

Parameter	Unit	L4 Spec.	DESY	ISIS	SNS	BNL
Beam energy	keV	*45*	35	17–35	65	35, 40
Pulse duration	ms	*0.4*	0.1	0.5	1.	0.8
Repetition rate	Hz	*2*	6	50	60	6.6
H^- current	mA	*40/80*	30	35	60	65, 100
H^- production mode			Volume	Cs-Arc	Cs-surface	Cs-surface
Plasma heating:		*RF*	RF	Penning	RF	Magnetron
$Emittance_{Norm\ RMS}$	mm mrad	*0.25*	0.25	0.2	0.25	0.4, 0.56
Cs-consumption	mg/day		0	100	<1	12
Operation MTBM	weeks	*50*	50	5	6	36

operation. A 100 kW, 2 MHz RF amplifier developed at CERN will be used for both sources. The only system producing routinely 80 mA H^- current is BNL's Magnetron [12], however within a larger emittance than specified by Linac4; therefore, this production mode is the backup option in case the SNS-type source could not provide the design intensity. A summary of the main parameters of existing H^- ion sources is given in Table 2. The Cs consumption normalized to the H^- beam current is lowest for the SNS caesiated surface production systems.

The challenge of the Linac4 ion source is to design and produce a 45 kV volume H^- source for the tests of the 3MeV section and a caesiated surface ion source prototype operating at the 0.1% duty factor required for Linac4 operation [15]. Operation and measurement of ion sources performance is foreseen in stages (20 mA, 40 mA and maximum H^- current). The layout of the ion source is shown in Fig. 3 and the details of the plasma generators of a volume and a caesiated surface source are illustrated in Fig. 4.

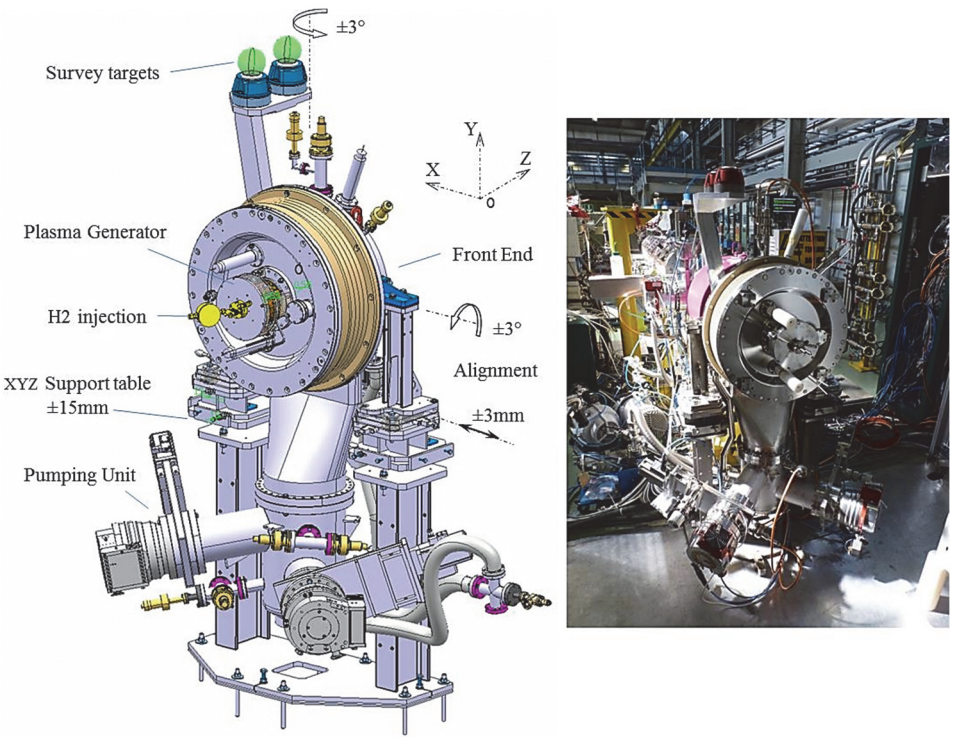

Fig. 3. Layout of the Linac4 ion source (volume production version) and its dedicated turbo-molecular pumping unit; the front end is installed on an adjustable support table. Once aligned, beam based minor offset of the horizontal position and angular orientations can be corrected. The plasma generator and beam extraction electrodes are mounted on an exchangeable flange.

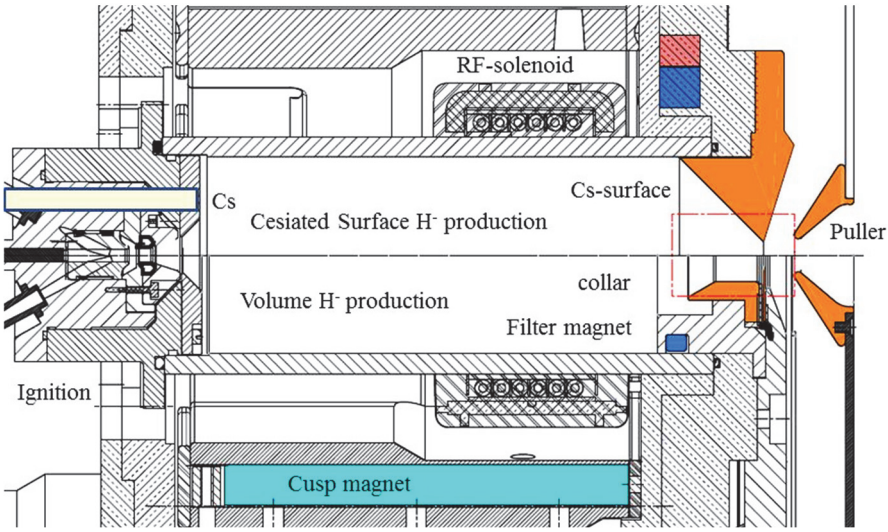

Fig. 4. Comparative schemes of plasma generators dedicated to cesiated surface (top) and volume production of H^- ions. The extraction geometry (diameter of the extraction hole and geometry of the puller) is similar to compare easily simulation and measurement conditions. The plasma-beam-formation region simulated in [24] is illustrated by a red dotted line.

After commissioning of the prototypes, the priority will be to characterize the plasma parameters best suited for H^- production, to measures the figures of merit of reliability and stability, identify the driving factors of the Mean Time Between Maintenance MTBM and minimize down time or ion source exchange/ restart time. Depending on these findings, minimization of the emittance growth will motivate a 2nd order iteration of the design.

Modeling and simulation of the various physical and chemical processes involved in the H^- production must be complemented by dedicated experimental techniques and measurement campaigns. Observables are mandatory to validate the design and to further optimize the design; on-going simulation, control and experimental tasks are summarized in the next sections.

H_2-injection: The base line selected is a piezo valve driven pulsed injection into the plasma chamber. The dynamics of the flow from the injection line (0.3 to 2.5 bar, stabilized to 0.1%) down to below 10^{-6} mbar in the pumping system was simulated by electrical equivalent circuits [16] and calibrated [17].

RF-coupling: At plasma ignition, the electron/proton density ramps from 0 to typically 10^{18} m^{-3} within few tens of micro seconds. The plasma is ignited either via arc discharge or capacitive coupling; it is then sustained by inductive coupling of the RF-injected power into the plasma. The RF amplifier and matching circuit

are engineered to follow in real time major changes of the load while being constantly matched via constant adaptation of the frequency [18]. The RF power and frequency are driven by arbitrary functions and plasma ignition is time tagged via an intensity threshold of the optical light emitted from the plasma.

Plasma: The hydrogen plasma is confined in a ceramic chamber surrounded by a permanent octupole magnet cusp in Halbach configuration. In the plasma expensing region, a magnetic dipole field reduces the electron energy in the vicinity of the beam extraction hole. The plasma is characterized by its neutrals and H^-/proton/electron densities, electron temperature and distribution of the excitation levels of the hydrogen atoms and molecules. Langmuir gauge measurements of the electron energy distribution function and plasma density [19] are complementary to non-invasive photometry and spectrometry [20] that provide on-line observables that must be correlated to plasma modeling (i.e. collision-radiation model) via Particle in Cell simulation. Preliminary simulation results at low plasma density [21] illustrate the pulsing of the plasma and the effect of the cusp field on the average electron energy.

Pulsed High Voltage: Minimization of the HV-sparks induced damages observed on cw high voltages stabilized by capacitor banks motivated the choice of pulsed power supplies. The high voltage system includes a low voltage electron dump (0–10 kV), a puller electrode (20–30 kV) extracting the beam and a high voltage (40–50 kV) acceleration station (or ground electrode?) defining the beam energy. The pulsed HV-system is based on standard power converters feeding dedicated HV-transformers located in the vicinity of the ion source [22]. It is specified to provide fast ramps and a 0.7 ms flat top held at nominal voltage under the pulsed H^- and electron beam loads. Furthermore, current limits allow identifying overcurrent and switching off the HV within a few micro seconds.

Beam formation: The beam formation region is composed of puller, electron dump and ground electrodes. Electrodes geometries and voltages must be optimized for the H^- beam and co-extracted electron currents [23]. The electron to H^- ratio is driven by the plasma parameters at the extraction hole and the extraction field; rather difficult to predict it must be measured to fine tune the space charge driven beam formation region. Particle in cell simulation of the beam formation region based on expected plasma parameters and puller geometries were achieved [24] for volume and surface production modes. An electrostatic accelerating Einzel lens matches the beam into the two solenoid Low Energy Beam Transport (LEBT) section.

4. Challenges of the 3 MeV Injector

The injector is the most critical part of any linear accelerator: this is where the particles are produced, where the beam emittance is generated, where the Coulomb repulsion between particles is the highest requiring particular focusing solutions, where the relativistic beta of the particles increases drastically imposing the use of complex mechanical structures, and where safety and collimation system have to be placed, before the energy becomes too high forbidding any particle loss.

The Linac4 injector section is about 9 m long; made of the ion source, of a Low Energy Beam Transport (LEBT), of a Radio Frequency Quadrupole (RFQ) and of a chopping/matching transport line it brings the beam to the energy of 3 MeV, a value still below the activation limits for commonly used metals. The LEBT is of the 2-solenoid type, and includes beam stoppers, some diagnostics and a gas injection system to control beam neutralization. The RFQ (Fig. 5), a combined focusing-bunching-accelerating device of 3-m length is of the brazed-copper 4-vane type and has been entirely built in the CERN Workshop; the RFQ electrodes ("vanes") have been accurately brazed in position after a complex sequence of machining steps and thermal treatments intended to keep vane position errors after brazing within the 30 μm tolerance required by beam dynamics and adjustment of the RF field. The overall quadrupole field error is below ±1% [25].

The 3.6 m long chopping line that follows the RFQ houses two chopping structures, fast electrostatic deflectors capable of deflecting selected trains of bunches into a dump placed inside the line. The chopper will thus create beam free intervals within the linac current pulse at positions corresponding to the

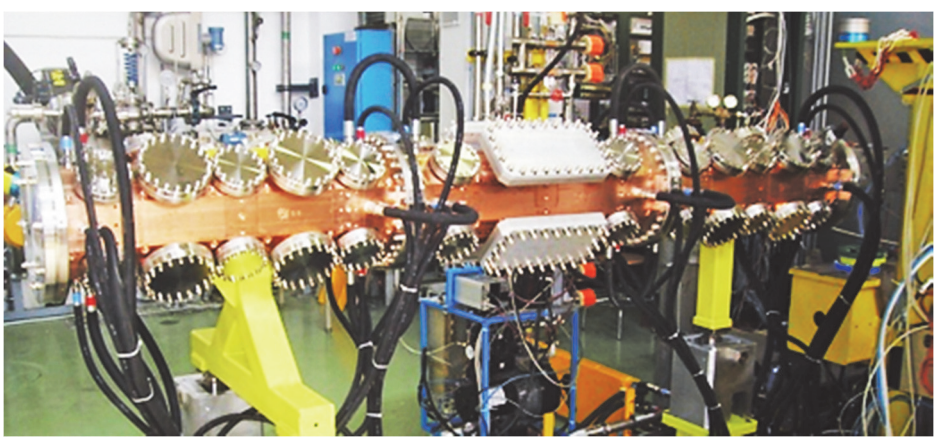

Fig. 5. The Linac4 RFQ.

transitions between the 2 MHz buckets in the PSB, where particles would be lost during the RF capture process. The choppers are 40 cm long meander-line deflectors mounted on a ceramic substrate and inserted into a quadrupole. Pulses of >650 V with rise times of 1.5 ns (10 to 90%) have been produced during testing, a value that allows the chopper voltage to rise between two 352 MHz bunches thus avoiding partially deflected bunches [26]. The deflected beam is sent on a conical dump that acts like a collimator for the non-deflected beam. Three rebunching cavities, 11 quadrupoles and diagnostic equipment complete the chopper line and allow transporting, measuring and matching of the beam before injection into the DTL.

5. Challenges of the Accelerating Structures

In the energy range between 3 MeV and 160 MeV the beam velocity and thus the basic geometrical period (proportional to $\beta\lambda$) increase by a factor 6.5; at the same time space charge defocusing decreases, allowing to progressively lengthening the focusing periods including an increasing number of geometrical periods. This broad range of mechanical and focusing parameters has to be covered with a series of different accelerating structures, each of them providing optimized mechanical configuration, RF efficiency (shunt impedance), and focusing for the beam energy range in which it operates. An additional constraint is the requirement to keep the same RF frequency up to the final energy, to standardize the RF system reducing cost and simplifying maintenance. A thorough optimization of the Linac4 accelerating section led to a design based on a sequence of three accelerating structures: a Drift Tube Linac (DTL), a Cell-Coupled Drift Tube Linac (CCDTL) and a Pi-Mode Structure (PIMS) [27].

The DTL is divided into three tanks and accelerates the beam up to 50 MeV. Focusing is provided by 108 Permanent Magnet Quadrupoles (PMQ) placed in vacuum inside the DTL drift tubes. A special mechanical design has been developed for the DTL, providing a precise positioning of the drift tubes inside the tank without using bellows or flexible vacuum joints to align the tubes after assembly [28]. Figure 6 shows the first segment of DTL Tank1 during low-power RF tests.

Although fully successful, the design of the DTL has confirmed that this structure remains complex and expensive to build; moreover, the fact that the quadrupole magnets are welded inside the drift tubes makes access for repair extremely difficult. For these reasons, as soon as the increase in energy of the beam permits longer distances between quadrupoles the Linac4 design adopts another type of structure, the Cell-Coupled DTL. In a CCDTL short DTL-like

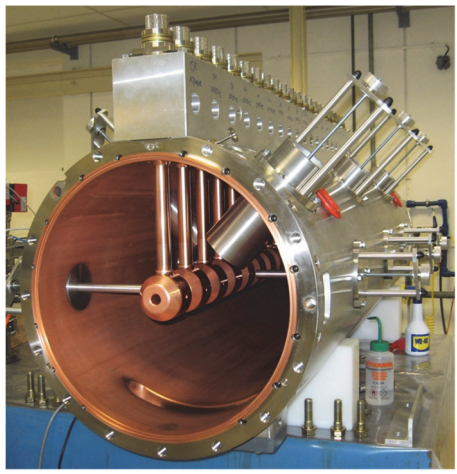

Fig. 6. DTL.

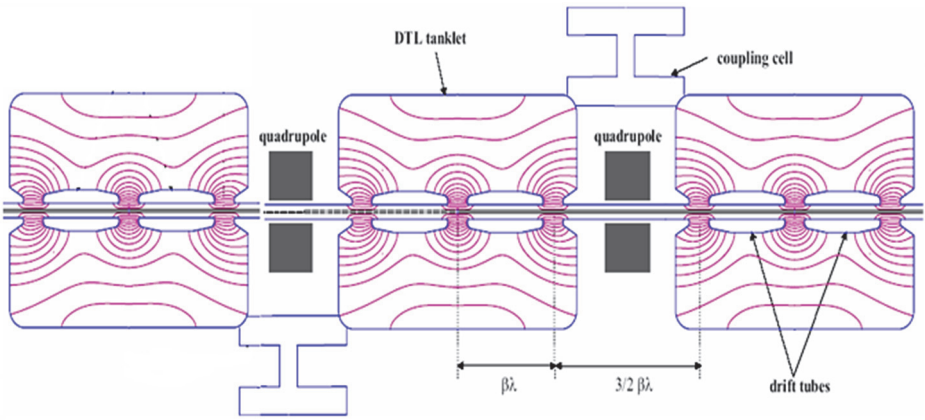

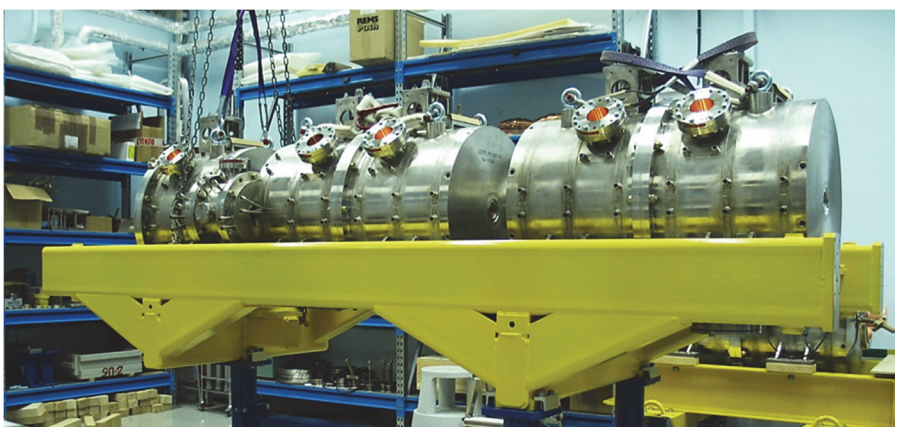

Fig. 7. CCDTL scheme (with electric field lines); module 2 during tests.

tanks are connected by coupling cells to form a single RF structure; the coupling cells leave space for placing the quadrupoles in an accessible position between the tanks and the fact that the drift tubes do not contain quadrupoles allows for smaller diameter tubes providing higher RF shunt impedance. The Linac4 CCDTL is made of 7 accelerating modules for a maximum RF power of 1 MW each, accelerating the beam to 104 MeV; a module is composed of 3 DTL-type tanks housing two drift tubes each plus two coupling cells [29]. Focusing is provided by a combination of PMQs (between tanks) and electromagnetic quadrupoles (between modules). Figure 7 shows the CCDTL principle and one of the modules produced for Linac4.

The third accelerating structure, called Pi-Mode Structure (PIMS), covers the energy range 104–160 MeV where focusing is required only between modules; here a module is composed of a single resonator made of seven cells coupled via slots and operating in π-mode [30]. In the PIMS section there are 12 modules of this type. The cells are made of copper and electron-beam welded. The first PIMS module is shown in Fig. 8.

Fig. 8. The first PIMS module under high-power tests.

6. Infrastructure and Operational Challenges

Linac4 is a modern linear accelerator that requires a complex infrastructure, housed in a large surface building above the machine tunnel. Particularly complex is the high-power Radio-Frequency system (Fig. 9), composed of thirteen 1.3-MW-klystrons, previously used in the CERN LEP accelerator, and six new klystrons of 2.8 MW, all operating in pulsed mode. The power out of the

2.8 MW klystrons is divided in two, allowing to either feed two couplers on the DTL tanks 2 and 3 or at high energy to feed two PIMS cavities in parallel. It is foreseen that as the stock of LEP klystrons runs out, pairs of LEP klystrons will be replaced by new klystrons equipped with a power splitter, leaving the waveguide network unchanged and progressively increasing the number of RF stations feeding two cavities [31]. The 110 kV modulators, equipped with a HV pulse transformer and a droop compensation bouncer, have a modular design that allows feeding of either one high-power klystron or two LEP-type units. A digital Low-Level RF derived from the LHC system and equipped with feed-forward capability is used to precisely set the cavity voltages.

Fig. 9. Linac4 klystron gallery.

Linac4 will have to face a number of challenges related to the operation as injector of the PSB and of the entire LHC injection chain. First of all, the reliability of the linac injector must be the highest of all accelerators in the chain; achieving beam availability levels around 98%, as is the case with Linac2, is a challenge in itself and requires a careful design of all components taking sufficient safety margins, with particular care in the design and margins of high voltage components, a preference for proven technical solutions, the selection of component architectures less prone to faults, a thorough testing of all components before installation in the linac, and finally a year-long reliability run before connection to the PSB.

Another important requirement for Linac4 is providing a beam perfectly adapted to the PSB in terms of beam quality, matched beam parameters, synchronization, and safe operation. The beam parameters in Linac4 are constantly monitored via a large number of beam diagnostics devices, often derived from standard units used in other machines at CERN and adapted for the reduced longitudinal space and the specific beam parameters of a linac. There are in Linac4 27 beam position monitors based on strip-line detectors. Beam profile along the machine is measured by 16 SEM-grids and 6 wire scanners and beam intensity by 15 beam current transformers [32]. The beam parameters before injection into the PSB are measured in two dedicated measurement lines, for transverse and longitudinal beam parameters. A complex interlock system protects the machine from damage coming from beam loss in the long multi-branch transport lines between Linac4 and the PSB.

References

[1] R. Garoby and M. Vretenar, Proposal for a 2 GeV Linac Injector for the CERN PS, PS/RF/Note 96-27.
[2] M. Benedikt *et al.*, The PS complex produces the nominal LHC beam, in *Proc. of EPAC 2000*, Vienna.
[3] M. Benedikt, K. Cornelis, R. Garoby, E. Métral, F. Ruggiero and M. Vretenar, Report of the High Intensity Protons Working Group, CERN-AB-2004-022-OP-RF.
[4] M. Vretenar (ed.), Conceptual Design of the SPL, a high-power superconducting Linac at CERN, CERN 2000-012.
[5] M. Vretenar, R. Garoby, K. Hanke, A.M. Lombardi, C. Rossi and F. Gerigk, Design of Linac4 a new injector for the CERN Booster, in *Proc. of 2004 Linac Conf.*, Lübeck.
[6] F. Gerigk, M. Vretenar (eds.), Linac4 Technical Design Report, CERN-AB-2006-084.
[7] Yu. I. Bel'chenko, G. I. Dimov and V. G. Dudnikov, *Doklady Akademii Nauk SSSR*, **213**, 1283 (1973).
[8] J. Lettry, J. Alessi, D. Faircloth, A. Gerardin, T. Kalvas, H. Pereira and S. Sgobba, Investigation of ISIS and BNL ion source electrodes after extended operation, *Review of Scientific Instruments* **83**, 02A728 (2012).
[9] H. Pereira, J. Lettry, J. Alessi and T. Kalvas, Estimation of Sputtering Damages on a Magnetron H^- Ion Source Induced by Cs^+ and H^+ Ions, *AIP Conf. Proc.* **1515**, 81–88 (2013).
[10] M. P. Stockli, B. X. Han, S. N. Murray, T. R. Pennisi, M. Santana and R. Welton, Recent performance of the SNS H^- source for 1-MW neutron production, *AIP Conf. Proc.* **1515**, 292 (2013).
[11] R. F. Welton, N. J. Desai, B. X. Han, E. A. Kenik, S. N. Murray Jr., T. R. Pennisi, K. G. Potter, B. R. Lang, M. Santana and M. P. Stockli, Ion source development at the SNS, *AIP Conf. Proc.* **1390**, 226–234 (2013).

[12] J. Alessi, in *Proc. of 20th ICFA Advanced Beam Dynamics Workshop on High Intensity and High Brightness Hadron Beams*, 2002.
[13] J. Peters, The HERA Volume H^- Source, in *Proc. of PAC05*, TPPE001, p. 788 (2005).
[14] D. C. Faircloth, J. W. G. Thomason, M. O. Whitehead, W. Lau and S. Yang, *Review of Scientific Instruments* **75**(5), 1735 (2004).
[15] J. Lettry, D. Aguglia, Y. Coutron, A. Dallochio, H. Perreira, E. Chaudet, J. Hansen, E. Mahner, S. Mathot, S. Mattei, O. Midttun, P. Moyret, D. Nisbet, M. O'Neil, M. Paoluzzi, C. Pasquino, J. Sanchez Arias, C. Schmitzer, R. Scrivens, D. Steyaert and J. Gil Flores, H^- ion sources for CERN's Linac4, *AIP Conf. Proc.* **1515**, 302–311 (2013).
[16] C. Pasquino, P. Chiggiato, A. Michet, J. Hansen and J. Lettry, Vacuum simulation and characterisation for the LINAC4 H^- source, *AIP Conf. Proc.* **1515**, 401–408 (2013).
[17] E. Mahner, J. Lettry, S. Mattei, M. O'Neil, C. Pasquino and C. Schmitzer, Gas injection and fast-pressure-rise measurements for the Linac 4 H^- source, *AIP Conf. Proc.* **1515**, 425–432 (2013).
[18] M. Paoluzzi, M. Haase, J. Marques Balula and D. Nisbet, CERN LINAC4 H^- Source and SPL plasma generator RF systems, RF power coupling and impedance measurements, *AIP Conf. Proc.* **1390**, 265–271 (2011).
[19] C. Schmitzer, M. Kronberger, J. Lettry, J. Sanchez-Arias and H. Störi, Plasma characterization of the SPL plasma chamber using a 2 MHz compensated Langmuir Probe, *Review of Scientific Instruments* **83**, 02A715 (2012).
[20] J. Lettry, U. Fantz, M. Kronberger, T. Kalvas, H. Koivisto, J. Komppula, E. Mahner, C. Schmitzer, J. Sanchez, R. Scrivens, O. Midttun, P. Myllyperkiö, M. O'Neil, H. Pereira, M. Paoluzzi, O. Tarvainen and D. Wünderlich, Optical Emission Spectroscopy of the Linac4 and SPL Plasma Generators, *Review of Scientific Instruments* **83**, 02A729 (2012).
[21] S. Mattei, M. Ohta, A. Hatayama, J. Lettry, Y. Kawamura, M. Yasumoto and C. Schmitzer, Plasma modeling of the Linac4 H^- ion source, *AIP Conf. Proc.* **1515**, 386–393 (2013).
[22] D. Aguglia, Design of a System of High Voltage Pulsed Power Converters for CERN's Linac4 H^- Ion Source, to be presented at the IEEE Pulsed Power & Plasma Science International conference, San Francisco (USA), 12–16 June 2013.
[23] Ø. Midttun, T. Kalvas, M. Kronberger, J. Lettry and R. Scrivens, A magnetized Einzel-lens electron dump for the Linac4 H^- ion source, *AIP Conf. Proc.* **1515**, 481–490 (2013).
[24] S. Mochalskyy, J. Lettry, T. Minea, A. F. Lifschitz, C. Schmitzer, O. Midttun and D. Steyaert, Numerical modeling of the Linac4 negative ion source extraction region by 3D PIC-MCC code ONIX, *AIP Conf. Proc.* **1515**, 31–40 (2013).
[25] C. Rossi, L. Arnaudon, G. Bellodi, J. Broere, O. Brunner, A. M. Lombardi, J. Marques Balula, P. Martinez Yanez, J. Noirjean, C. Pasquino, U. Raich, F. Roncarolo, M. Vretenar, M. Desmons, A. France and O. Piquet, Commissioning of the Linac4 RFQ at the 3 MeV Test Stand, in *Proc. of IPAC 2013*, Shanghai.
[26] M. Paoluzzi, A fast 650V chopper driver, in *Proc. of IPAC 2011*, San Sebastian.

[27] F. Gerigk, N. Alharbi, M. Pasini, S. Ramberger, M. Vretenar and R. Wegner, RF Structures for Linac4, in *Proc. of 2007 PAC*, Albuquerque.
[28] S. Ramberger, G. De Michele, F. Gerigk, J. M. Giguet, J. B. Lallement, A. M. Lombardi and M. Vretenar, Production design of the Drift Tube Linac for the CERN Linac4, in *Proc. of 2010 Linac Conf.*, Tsukuba.
[29] M. Vretenar, Y. Cuvet, G. De Michele, F. Gerigk, M. Pasini, S. Ramberger, R. Wegner, E. Kenjebulatov, A. Kryuchkov, E. Rotov and A. Tribendis, Development of a Cell-Coupled Drift Tube Linac for Linac4, in *Proc. of 2008 Linac Conf.*, Victoria.
[30] F. Gerigk, P. Ugena Tirado, J. M. Giguet and R. Wegner, High Power Tests of the first PIMS Cavity for Linac4, in *Proc. of IPAC 2011*, San Sebastian.
[31] O. Brunner, N. Schwerg and E. Ciapala, RF Power Generation in Linac4, in *Proc. of 2010 Linac Conf.*, Tsukuba.
[32] F. Roncarolo *et al.*, Overview of the CERN Linac4 Beam Instrumentation, in *Proc. of 2010 Linac Conf.*, Tsukuba.